THE EFFECT OF TRACK IRREGULARITY AND WHEEL LOAD ON THE DYNAMIC RESPONSE OF A HIGH-SPEED RAIL SYSTEM

Tran Minh Thi, Kok K. Ang
Department of Civil Engineering, National University of Singapore, Singapore 117576, Singapore, email: ceeangkk@nus.edu.sg (K.K. Ang)

Luong Van Hai
Faculty of Civil Engineering, Ho Chi Minh City University of Technology, VNU HCMC, Vietnam

ABSTRACT

In this paper, a computational study using the moving element method (MEM) was carried out to investigate the dynamic response of a high-speed rail (HSR). A new formulation for calculating the structural matrices of the moving element is proposed. Two wheel-rail contact problems will be examined. One is linear and the other nonlinear. A parametric study is carried out to understand the effects of various factors on the response of the train-track system such as the severity of railhead roughness and the wheel load. In particular, the effect of above factors on the occurrence of the jumping wheel phenomenon, which occurs when there is a momentary loss of contact between the wheel and track, is considered.

Keywords: Moving element method, constant and varying velocities, wheel-rail interaction, track irregularity.

Introduction

Railway transportation is one of the key modes of travel today. The advancement in train technology leading to faster and faster trains is without doubt a positive development, which makes high-speed rails (HSRs) more attractive as an alternative to other modes of transportation for long distance travel.

The HSR has been investigated as a track beam resting on a visco-elastic foundation subject to moving loads varying both in time and space. For example, as early as 1974, Timoshenko [1] derived the solutions for the dynamic analysis of a simply supported beam resting on a Winkler foundation subject to moving loads by means of the mode superposition method. Mathews [2] and Jazequel [3] studied the problem using Fourier Transformation Method (FTM). The FTM may give accurate solutions but becomes cumbersome when dealing with complicated coupled system, such as multi-degrees of freedom system with multiple contact points or where there are moving loads that involve acceleration/ deceleration. The Finite Element Method (FEM) is well established and known to solve many complicated problems. Many researchers, such as Filho [4], Hino [5] and Olsson [6], have adopted the FEM to determine the dynamic response of simply supported beams subject to moving constant loads.

Various researchers have investigated the problem of loads travelling at non-uniform velocities. Suzuki [7] employed

the energy method to derive the governing equation of a finite beam subject to traveling loads involving acceleration. Involved integrations are carried out using Fresnel integrals and analytical solutions are presented. The vibration response of a train-track-foundation system resulting from a vehicle travelling at variable velocities has been investigated by Yadav [8]. Analytical solutions were obtained and the response characteristics of the system were examined. Karlstrom [9] used an analytical approach to investigate ground vibrations due to accelerating and decelerating trains. The solution is based on Fourier transforms in time and along the track.

In dealing with moving load problems, the FEM encounters difficulty when the moving load approaches the boundary of the finite domain and travels beyond the boundary. These difficulties can be overcome by employing a large enough domain size but at the expense of significant increase in computational time. In an attempt to overcome the complication encountered by FEM, Krenk et al. [10] proposed the use of FEM in convected coordinates to obtain the response of an elastic half-space subject to a moving load. The key advantage enjoyed by this approach is its ability to overcome the problem due to the moving load travelling over a finite domain. Andersen et al. [11] gave an FEM formulation for the problem of a beam on a Kelvin foundation subject to a harmonic moving load. Koh et al. [12] adopted the idea of convected coordinates for solving train-track problems, and named the numerical algorithm as moving element method (MEM). The method was subsequently applied to the analysis of in-plane dynamic response of annular disk [13] and moving loads on a viscoelastic half space [14]. Recently, Ang et al. [15] applied the MEM to investigate the "jumping wheel" phenomenon in high-speed train motion at constant velocity over a transition region where there is a sudden change of foundation stiffness. The phenomenon occurs when there is momentary loss of contact between train wheel and track. The effects of various key parameters such as speed of train, degree of track irregularity and degree of change of foundation stiffness at the transition region were examined.

This paper is concerned with a computational study of the dynamic response of HSR systems moving at constant and varying speeds using the MEM. A new formulation for calculating the structural matrices of the moving element is proposed. Parametric study is performed to understand the effects of various factors on the response of the train-track system, such as the severity of railhead roughness and the wheel load. In particular, the effect of above factors on the occurrence of the jumping wheel phenomenon is considered. As the dynamic response of the track depends significantly on the contact force between wheel and track, this study is also concerned with examining the suitability of two contact models.

Formulation and methodology

The HSR system comprises of a train traversing over a rail beam in the positive x-direction. The origin of the fixed x-axis is arbitrarily located along the beam. However, for convenience, its origin is taken such that the train is at $x = 0$ when $t = 0$. The velocity and acceleration of the train at any instant are v and a, respectively. The railhead is assumed to have some imperfections resulting in the so-called "track irregularity". The moving sprung-mass model, as shown in Figure 1, is employed to model the train. The topmost mass m_1 represents the car body where the passengers are. The car body is

supported by the bogie of mass m_2 through a secondary suspension system modeled by the spring k_1 and dashpot c_1. The bogie is in turn supported by the wheel-axle system of mass m_3 through a primary suspension system modeled by the spring k_2 and dashpot c_2. The contact between the wheel and rail beam is modeled by the spring k_3 and dashpot c_3. The rail beam rests on a viscoelastic foundation comprising of vertical springs $\bar{k}$ and dashpots $\bar{c}$. The vertical displacement of the track is denoted by y, while the vertical displacements of the car body, bogie and wheel-axle are denoted by u_1, u_2 and u_3, respectively.

Figure 1. Moving sprung-mass model by Koh et al. [12]

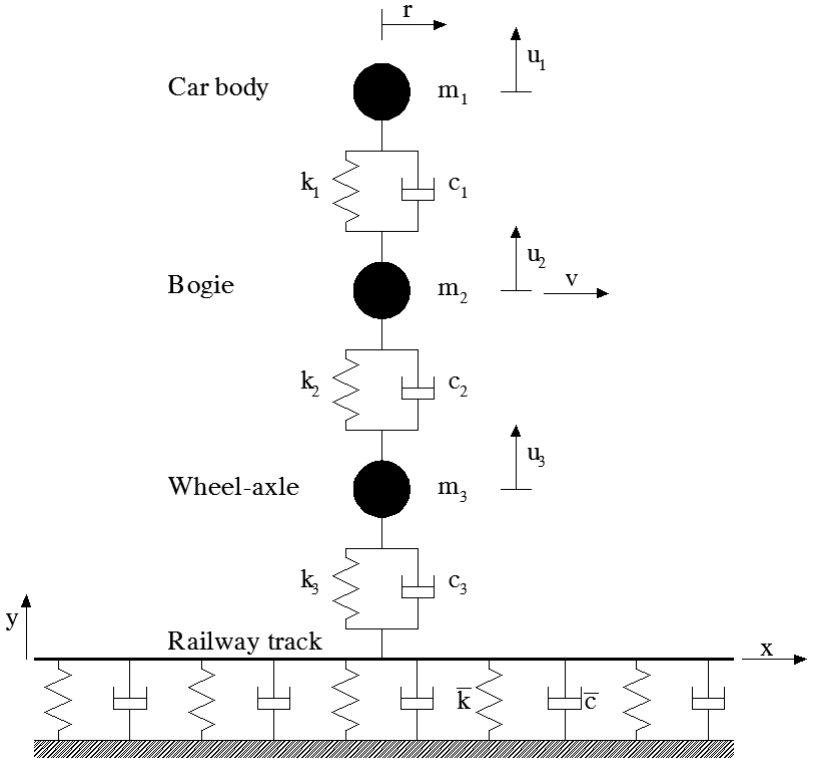

The governing equation of motion of the rail beam, which is modeled as an Euler-Bernoulli beam resting on a viscoelastic foundation subject to a moving train load, is given by

$$EI\frac{\partial^4 y}{\partial x^4}+\bar{m}\frac{\partial^2 y}{\partial t^2}+\bar{c}\frac{\partial y}{\partial t}+\bar{k}y=F_c\delta(x-s) \quad (1)$$

where E, I and $\bar{m}$ are the Young's modulus, second moment of inertia, mass per unit length of the rail beam, respectively; t denotes time; F_c the dynamic contact force exerted between the wheel and track; s the distance traveled by the train at any instant t; and δ the Dirac-delta function.

The moving element method was first proposed with the idea of attaching the origin of the spatial coordinates system to the applied point of the moving load. Figure 2 shows a travelling r-axis moving at the same speed as the moving load. The relationship between the moving coordinate r and the fixed coordinate x is given by

$$r=x-s \quad (2)$$

Figure 2. Coordinate systems for moving load problem

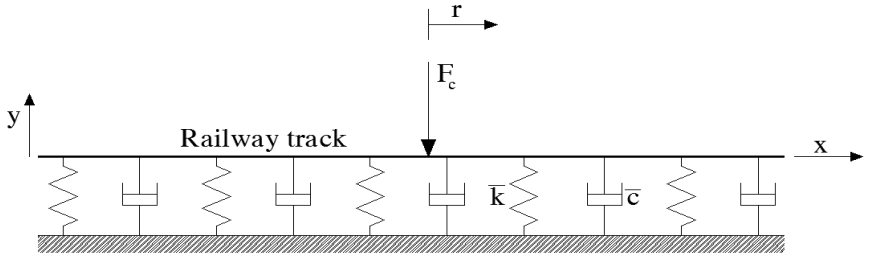

In view of Eq. (3), the governing equation in Eq. (1) may be rewritten as

$$EI\frac{\partial^4 y}{\partial r^4}+\bar{m}\left(v^2\frac{\partial^2 y}{\partial r^2}-2v\frac{\partial^2 y}{\partial r\partial t}-a\frac{\partial y}{\partial r}+\frac{\partial^2 y}{\partial t^2}\right)+\bar{c}\left(\frac{\partial y}{\partial t}-v\frac{\partial y}{\partial r}\right)+\bar{k}y=F_c\delta(r) \tag{3}$$

By adopting Galerkin's approach and procedure of writing the weak form in term of the displacement field, the formulation for general mass $\mathbf{M}_e$, damping $\mathbf{C}_e$ and stiffness $\mathbf{K}_e$ matrices of the moving element can be proposed:

$$\begin{aligned}
\mathbf{M}_e &= \bar{m}\int_0^L \mathbf{N}^{\mathrm{T}}\mathbf{N}\,\mathrm{d}r \\
\mathbf{C}_e &= -2\bar{m}v\int_0^L \mathbf{N}^{\mathrm{T}}\mathbf{N}_{,r}\,\mathrm{d}r+\bar{c}\int_0^L \mathbf{N}^{\mathrm{T}}\mathbf{N}\,\mathrm{d}r \\
\mathbf{K}_e &= EI\int_0^L \mathbf{N}_{,rr}^{\mathrm{T}}\mathbf{N}_{,rr}\,\mathrm{d}r+\bar{m}v^2\int_0^L \mathbf{N}^{\mathrm{T}}\mathbf{N}_{,rr}\,\mathrm{d}r-\left(\bar{m}a+\bar{c}v\right)\int_0^L \mathbf{N}^{\mathrm{T}}\mathbf{N}_{,r}\,\mathrm{d}r+\bar{k}\int_0^L \mathbf{N}^{\mathrm{T}}\mathbf{N}\,\mathrm{d}r
\end{aligned} \tag{4}$$

where $(\ )_{,r}$ denotes partial derivative with respect to r and $(\ )_{,rr}$ denotes second partial derivative with respect to r. For beam elements, it is common to use the shape function $\mathbf{N}$ based on Hermitian cubic polynomials.

Considering the special case in which the train traverses at a constant velocity V, i.e. $a=0, v=V$, Eq. (4) reduces to

$$\begin{aligned}
\mathbf{M}_e &= \bar{m}\int_0^L \mathbf{N}^{\mathrm{T}}\mathbf{N}\,\mathrm{d}r \\
\mathbf{C}_e &= -2\bar{m}V\int_0^L \mathbf{N}^{\mathrm{T}}\mathbf{N}_{,r}\,\mathrm{d}r+\bar{c}\int_0^L \mathbf{N}^{\mathrm{T}}\mathbf{N}\,\mathrm{d}r \\
\mathbf{K}_e &= EI\int_0^L \mathbf{N}_{,rr}^{\mathrm{T}}\mathbf{N}_{,rr}\,\mathrm{d}r+\bar{m}V^2\int_0^L \mathbf{N}^{\mathrm{T}}\mathbf{N}_{,rr}\,\mathrm{d}r-\bar{c}V\int_0^L \mathbf{N}^{\mathrm{T}}\mathbf{N}_{,r}\,\mathrm{d}r+\bar{k}\int_0^L \mathbf{N}^{\mathrm{T}}\mathbf{N}\,\mathrm{d}r
\end{aligned} \tag{5}$$

It can be seen that the element mass, damping and stiffness matrices derived in Eq. (5) are identical to the matrices derived by Koh et al. [12].

In general, the wheel contact force F_c may be written as

$$F_c=c_3\Delta\dot{y}+k_3\Delta y \tag{6}$$

where the overdot operator denotes differentiation with respect to time and Δy the indentation at the contact surface which can be expressed as

$$\Delta y=y_r+y_t-u_3 \tag{7}$$

in which y_r and u_3 denote the

displacements of the rail and wheel, respectively, and y_t the magnitude of the track irregularity at the contact point. Note that track irregularity is a major source of the dynamic excitation. According to the recommendation by Nielsen [16], the track irregularity profile can be written in terms of a sinusoidal function as follows

$$y_t = -a_t \sin\frac{2\pi x}{\lambda_t} \tag{8}$$

where a_t and λ_t denote the amplitude and wavelength of the track irregularity, respectively.

As the dynamic response of the train-track system depends significantly on the accuracy in modeling the contact between the wheel and track, this study will evaluate two contact models. In these models, Hertz contact theory [17] is employed to account for the nonlinear contact force F_c between the wheel and rail as follows

$$\text{where } F_c = \begin{cases} K_H \Delta y^{\frac{3}{2}} & for \quad \Delta y \geq 0 \\ 0 & for \quad \Delta y < 0 \end{cases} \tag{9}$$

$$K_H = \frac{2}{3}\sqrt{\frac{E^2\sqrt{R_{wheel}R_{railprof}}}{(1-\upsilon^2)^2}} \tag{10}$$

in which K_H denotes the Hertzian spring constant; R_{wheel} and $R_{railprof}$ the radii of the wheel and railhead, respectively, and υ the Poisson's ratio of the material.

To avoid high computational cost and complexity of the nonlinear contact problem, many researchers have adopted a simplified approach based on a linearized Hertz contact model in which F_c is given by

$$F_c = \begin{cases} K_L \Delta y & for \quad \Delta y \geq 0 \\ 0 & for \quad \Delta y < 0 \end{cases} \tag{11}$$

where K_L is the linearized Hertzian spring constant [1] computed as follows

$$K_L = \sqrt[3]{\frac{3E^2W\sqrt{R_{wheel}R_{railprof}}}{2(1-\upsilon^2)^2}} \tag{12}$$

in which it is assumed that the reaction force at the contact point equals to the self-weight of the upper structure W of the train-track system [17].

The governing equations for the vehicle model are

$$\begin{aligned} m_1\ddot{u}_1 + k_1(u_1-u_2) + c_1(\dot{u}_1-\dot{u}_2) &= -m_1 g \\ m_2\ddot{u}_2 + k_2(u_2-u_3) + c_2(\dot{u}_2-\dot{u}_3) - k_1(u_1-u_2) - c_1(\dot{u}_1-\dot{u}_2) &= -m_2 g \\ m_3\ddot{u}_3 - k_2(u_2-u_3) - c_2(\dot{u}_2-\dot{u}_3) &= -m_3 g - F_c \end{aligned} \tag{13}$$

where g denotes gravitational acceleration. Upon combining Eq. (13) with the governing equations for the rail beam given in Eq. (3), the equation of motion for the train-track system may be written as

$$\mathbf{M}\ddot{\mathbf{z}} + \mathbf{C}\dot{\mathbf{z}} + \mathbf{K}\mathbf{z} = \mathbf{P} \tag{14}$$

where $\ddot{\mathbf{z}}$, $\dot{\mathbf{z}}$, $\mathbf{z}$ denote the global acceleration, velocity and displacement vectors of the train-track system, respectively; $\mathbf{M}$, $\mathbf{C}$ and $\mathbf{K}$ the global mass, damping and stiffness matrices, respectively; and $\mathbf{P}$ the global load vector. The above dynamic equation can be solved by any direct integration methods such as Newmark-β method [18].

Numerical results

To verify the accuracy of the proposed MEM approach in obtaining the dynamic response of a high-speed rail (HSR) considering variable train velocity, the present solutions are compared against solutions obtained by Koh et al. [12] using

the so-called 'cut-and-paste' FEM. The latter involves updating the force and displacement vectors in accordance with the position of the vehicle while keeping the structure mass, damping and stiffness matrices constant.

Table 1. Parameters for track-foundation model

Parameter	Value	Parameter	Value
Flexural stiffness	6.12×10^6 N m^2	Stiffness of foundation	1×10^7 N/m^2
Track section	UIC 60 (60 E1)	Damping ratio	0.1

For the purpose of comparison only, the same train speed profile adopted by Koh et al. [12] is employed. This speed profile is shown in Figure 3 where it can be seen that there are 3 phases of travel. The initial phase considers the train to be moving at a constant acceleration of travel and reaching a maximum speed of 20 m/s after 2 s. This is followed by the train travelling at the maximum constant speed for another 2 s during the second phase. In the final phase, the train decelerates at a constant magnitude to come to a complete halt after another 2 s of travel. Values of parameters related to the properties of track and foundation are summarized in Table 1 [12]. Results obtained using the proposed method are found to be in excellent agreement with those obtained by the 'cut-and-paste' FEM. Figure 4 shows the displacement time history of the wheel obtained by the two methods. In view there is virtually no visible difference in the plots obtained by both methods, no other comparison plots are thus presented. Note that the 'cut-and paste' FEM approach requires that all the finite elements are identical in length in order for the 'cut' and 'paste' operations to work properly.

Figure 3. Profile of train speed for comparison purpose

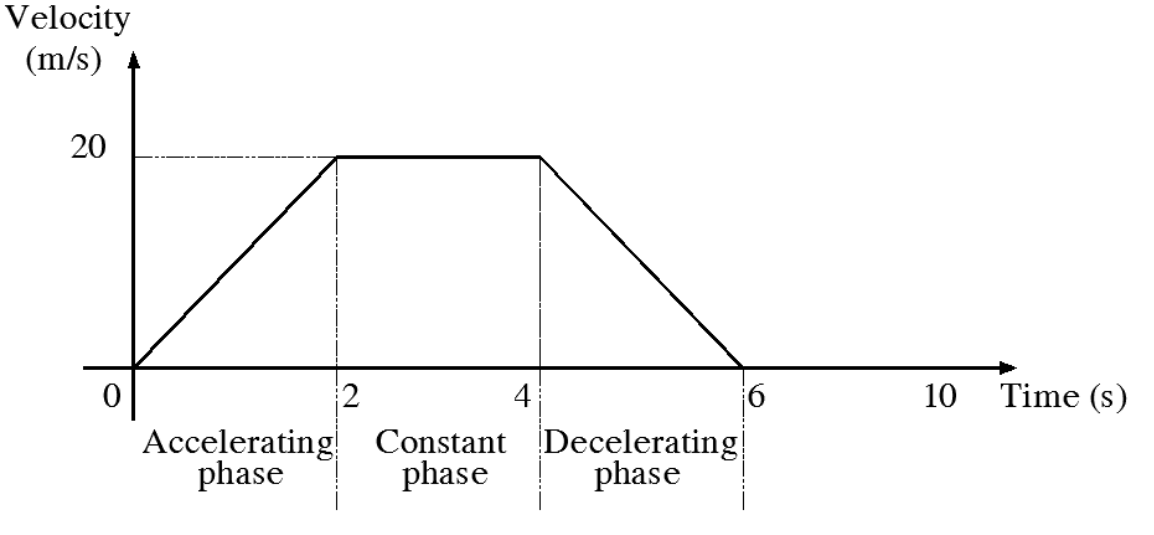

Figure 4. Comparison of wheel displacements between present study and Koh et al. (2003)

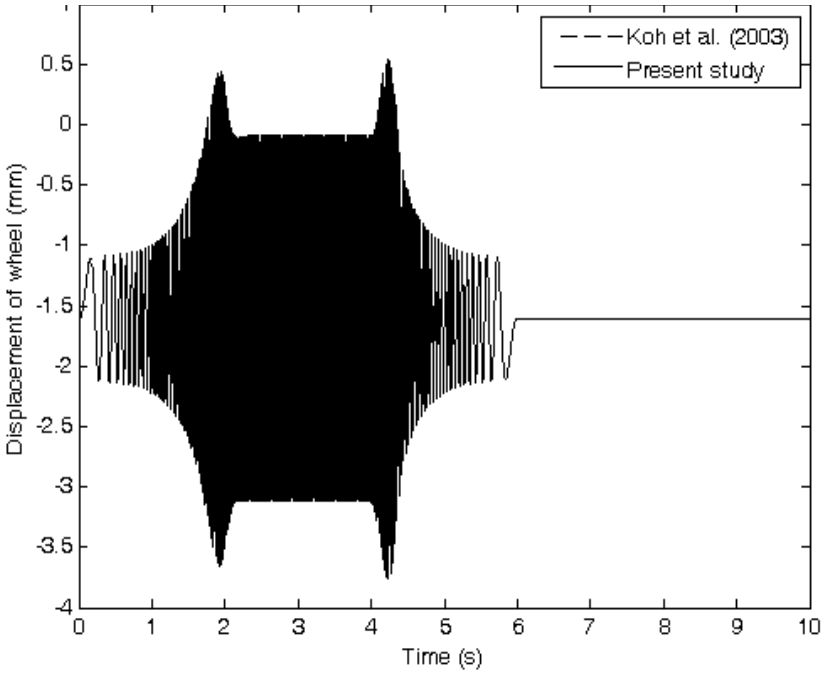

In the following sections, results from the study of HSR using the proposed MEM approach are presented. The case studies the response of high-speed train moving over a uniform Winkler foundation at constant speed. The effects of track irregularity and wheel load on the dynamic response of train-track system will be investigated using the Hertz nonlinear and linearized contact models. In the second case, the response of train-track system moving at varying speed will be investigated. The aim of this study is to determine the effects of track irregularity and wheel load on the occurrence of the jumping wheel phenomenon and dynamic response of the system during the accelerating or decelerating phases.

Case 1: Train travels at constant speed

The MEM model adopted in the study comprises of a truncated railway track of 50 m length discretized non-uniformly with elements ranging from a coarse 1 m to a more refined 0.1 m size. Note that refined element sizes are employed in the vicinity of the moving train load in order to capture accurately the maximum response of the train-track system. The equations of motion are solved using Newmark's constant acceleration method employing a time step of 0.0005s. This small time step size is necessary in view of the inherent high natural frequency of the train-track system. Values of parameters related to the properties of track and foundation are summarized in Table 1 [12]. In analyses involving the Hertz nonlinear contact model, Newton-Raphson's method [18] is employed to solve the resulting nonlinear equations of motion. Note that the radii of the wheel R_{wheel}, railhead $R_{railprof}$ and the Poisson's ratio of the wheel/rail material υ used in determining the nonlinear and linearized Hertz spring constants are taken to be 460 mm, 300 mm and 0.3, respectively. The wavelength of all track irregularities considered is taken to be 0.5 m. In reality, there is a varying range of wheel loads. Typical passenger vehicles range from about 40 to 60 kN while loaded vehicles have wheel loads in excess of 130 kN. Therefore, two wheel loads are

considered in the calculations, $W = 41$ kN for a lightest load [12] and 81 kN for an average passenger vehicle.

Figure 5, Figure 6 and Figure 7 show the variation of dynamic amplification factor (DAF) in wheel-rail contact force against track irregularity amplitude for various train speeds typically associated with today's HSR travels. All analyses are carried out twice, each using the nonlinear and linearized contact models. Note that DAF is defined as the ratio of the maximum dynamic contact force to the static wheel load which is the sum of the self-weights of car body, bogie and wheel-set. For the perfectly smooth ($a_t = 0$ mm) track, the DAF is found be 1. It means that the linearized contact spring properties computed in Eq. [12] according to the static wheel load condition [17] can be used. As to be expected, it can be seen that increasing amplitude of track irregularity and train speed has the effect of increasing the DAF. It also can be found that the DAF obtained using the linear contact model were found to agree well with those obtained by the nonlinear contact model at low vehicle speeds and small track irregularities. The well agreement also can be found at higher speeds when the amplitudes are smaller than 0.7 mm ($v = 70$ m/s) and 0.4 mm ($v = 90$ m/s). However, the difference between the DAFs given by the two contact models is no longer negligible at relatively high speeds and/or where there are significant track irregularities, i.e. the amplitudes are larger than 0.7 mm and 0.4 mm for train speed 70 m/s and 90 m/s, respectively. Therefore, the response of train-track system strongly depends on the irregularity amplitude and train speed. Also, the simpler linearized contact model is not suitable to account for the wheel-rail interaction when two above factors are not considered to be small enough.

These figures also show the effect of wheel load on the DAF of HSRs when increasing the track irregularity amplitude. It can be found that the lighter the wheel load is, the larger the DAF is. On physical nature, it is not surprising that the vibration of structure is large when the mass is small. Also, the DAF is found to be nearly 1.0 when the irregularity amplitudes are small than 0.1 mm for all cases. As the amplitude increases, the DAF is noted to increase rapidly with increasing train speed.

Figure 5. Effect of wheel load, track irregularity amplitude on the DAF (train speed is 50 m/s)

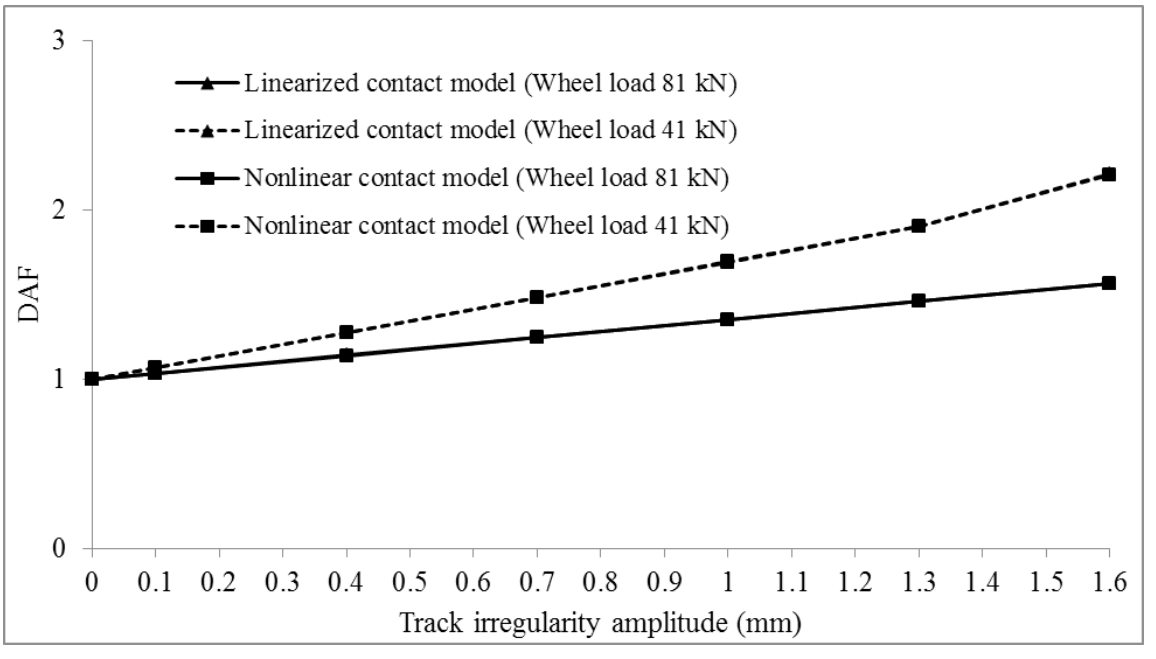

Figure 6. Effect of wheel load, track irregularity amplitude on the DAF (train speed is 70 m/s)

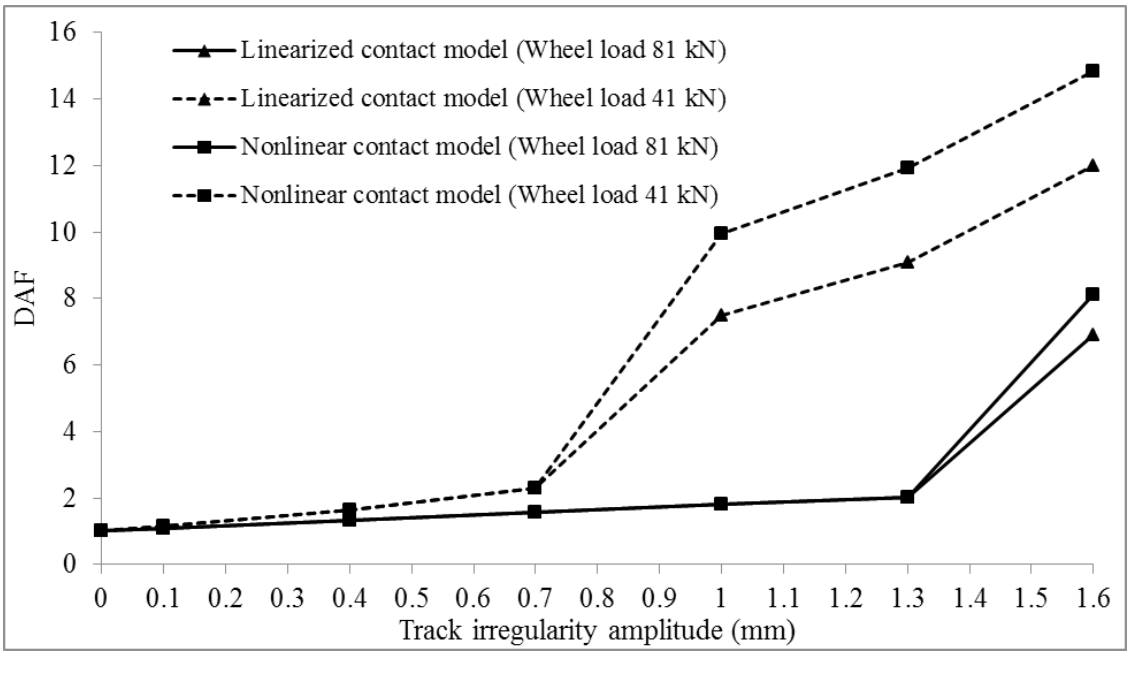

Figure 7. Effect of wheel load, track irregularity amplitude on the DAF (train speed is 90 m/s)

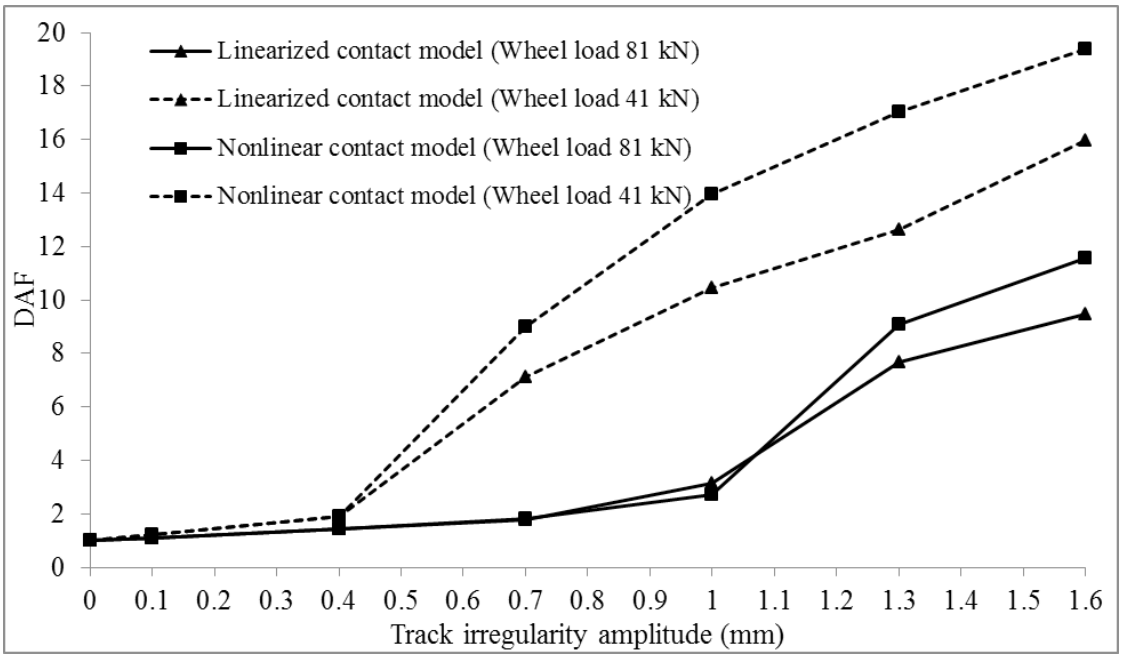

Moreover, the difference between two contact models also depends on the wheel load. Excellent agreement can be found at low vehicle speeds and small irregularity amplitudes. For higher train speed, the lighter the wheel load is, the larger the difference is. At low train speed, it can be seen that well agreements between two contact models are given in Figure 5. At higher train speed, the difference between two contact models depends strongly on track irregularity amplitude and wheel load. For lighter wheel load 41 kN, the difference between the DAFs given by the two contact models is larger than the one at higher wheel load for track irregularity amplitudes are larger than 0.7 mm. More details are given in Figure 6 and Figure 7. Also, at higher train speed and larger wheel load 81 kN, it can be seen that large difference between two contact models occurs at irregularity amplitudes 1.6 mm and 1.3 mm for train speed 70 m/s and 90 m/s, respectively.

Case 2: Train travels at varying speed

The proposed model adopted in the study comprises of a truncated railway track of 50 m length uniformly discretized into 250 moving finite elements. Using a time step of 0.0005s which is smaller than the recommended one-tenth the natural period of the rail beam on the Winkler foundation for a good compromise between accuracy of results and required computational effort, the equations of motion are solved using Newmark's constant acceleration method. Values of parameters related to the properties of track and foundation are summarized in Table 1 [12]. The Hertz nonlinear contact model is employed in this study. Solving the nonlinearity of contact equation, Newton-Raphson's method [18] is employed. Typical vehicle speed profile, as shown in Figure 8, is considered.

Figure 8. Profile of train speed

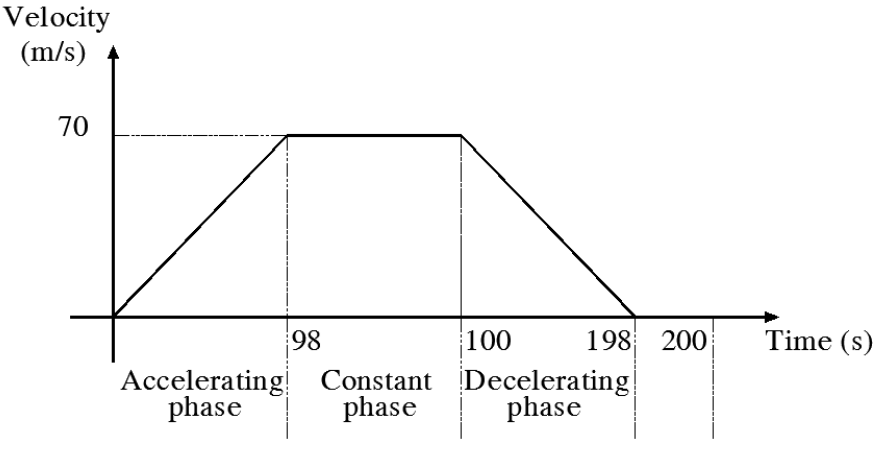

Figure 9 shows the effect of track irregularity amplitude and wheel load on the DAF in contact force, respectively. As the amplitude increases, the DAF is noted to increase rapidly with lighter wheel load, but the DAF almost do not change when wheel load is large. Note that the DAF is similar for all cases when the track irregularity amplitude is smooth. It is also interesting that the DAFs during the accelerating or and decelerating phases are always larger than ones during constant phase. Moreover, it can be found that the lighter the wheel load is, the larger the DAF is. On physical nature, it is not surprising when the vibration of structure is large because of the small mass. Clearly, the effect of the track irregularity and wheel load is significant on the design of the high-speed rail system when train travels at varying speed.

Figure 9. Effect of wheel load and track irregularity amplitude to DAF

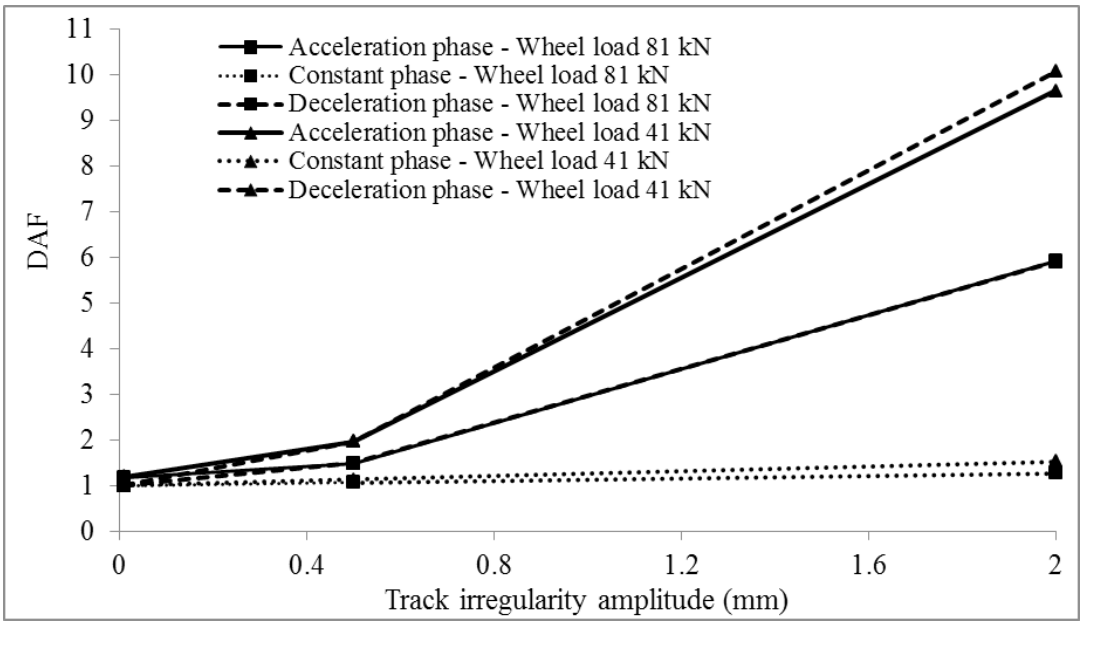

As aforementioned, the contact force between the wheel and rail strongly depends on track irregularity and wheel load. Therefore, these factors will also affect the jumping wheel phenomenon where there is the loss of contact between the wheel and rail. Using various train speeds, track irregularity amplitudes and wheel loads, Table 2 shows the occurrence or non-occurrence of the jumping wheel phenomenon which is denoted "N" or "Y", respectively. Note that three typical track irregularities with a wavelength of 1 m and the nonlinear contact model are only considered.

Table 2. Occurrence of the jumping wheel phenomenon

Phase	Track irregularity amplitude (mm)					
	0.01		0.5		2	
	Wheel load 41 kN	Wheel load 81 kN	Wheel load 41 kN	Wheel load 81 kN	Wheel load 41 kN	Wheel load 81 kN
Acceleration	N	N	N	N	Y	N
Constant	N	N	N	N	N	N
Deceleration	N	N	N	N	Y	N

As to be expected in considering low wheel load, when the small track irregularity amplitude is considered, the jumping wheel is unlikely to occur during all phases. It can be seen that the wheel easily jumps when the large track irregularity amplitude is studied during the accelerating or decelerating phases. For less large track irregularity amplitude, there is also a good possibility for the occurrence of the phenomenon. Considering high wheel load, it can be found that the jumping wheel phenomenon easily occurs during the accelerating or decelerating phases when the very large track irregularity amplitude is considered. In other cases, there is non-occurrence of the phenomenon. As compared with larger wheel load, it can be said that the smaller the wheel load, the easier the jumping wheel phenomenon is. It means that the result is reasonable to the real physical nature. It is necessary to control above factors to avoid the occurrence of the jumping wheel phenomenon for high-speed rail system, which is helpful for safety of passengers. Figure 10 shows typical contact forces between the wheel and rail when train travels at decelerating phase.

Figure 10. Effect of wheel load to contact force when train travels at decelerating phase

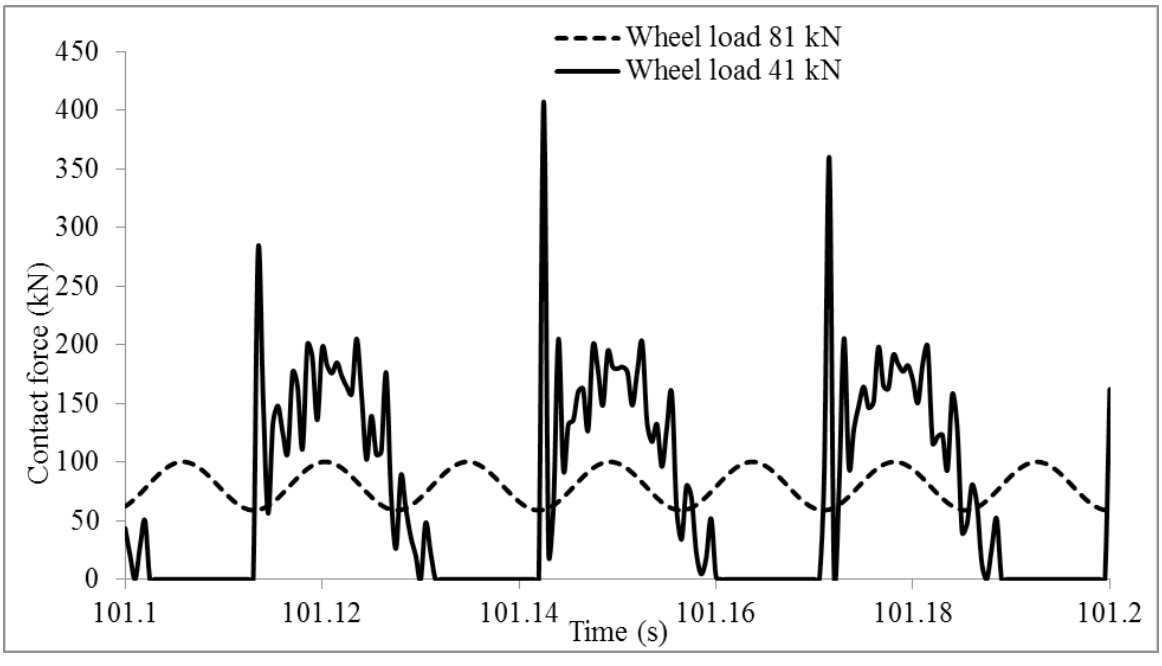

Conclusion

In this paper, a numerical study on the dynamic response of high-speed train-track system using the moving element method was carried out. A new and formulation for calculating the structural matrices of the moving element was proposed. Accounting for the wheel/rail interaction, the proposed linear and Hertz contact models were employed. The effects of track irregularity and wheel load on the response of high-speed rail system and 'jumping wheel' phenomenon are investigated.

The results obtained using the proposed MEM are agree well with available 'cut-and-paste' FEM. It is found that the DAF in contact force is more increasing when the irregularity amplitude is more increasing. Results obtained using the linear contact model were found to agree well with those obtained by the Hertz contact model at low vehicle speeds and small track irregularities. However, at relatively high speeds and/or where there are significant track irregularities, the difference between the results given by the two contact model is no longer negligible. It is reasonable to satisfy physical nature that the lighter the wheel load is, the larger the DAF is and the easier the jumping wheel phenomenon is.

Acknowledgments

This research is funded by Vietnam National University HoChiMinh City (VNU-HCM) under grant number B2013-20-07.

REFERENCES

[1] S. Timoshenko, D. H. Young, W. Jr. Weaver, Vibration Problems in Engineering, 4th ed., John Wiley, New York, 1974.

[2] P. M. Mathews, Vibrations of a beam on elastic foundation, Journal of Applied Mathematics and Mechanics, 38 (1958) 105-115.

[3] L. Jezequel, Response of Periodic Systems to a Moving Load, Journal of Applied

Mechanics 48 (1981) 613-618.

[4] F. V. Filho, Finite element analysis of structures under moving loads, Shock and Vibration Digest 10 (1978) 27-35.

[5] J. Hino, T. Yoshimura, N. Ananthanarayana, Vibration analysis of non-linear beams subjected to a moving load using the finite element method, Journal of Sound and Vibration 100 (4) (1985) 477-491.

[6] M. Olsson, Finite element, modal co-ordinate analysis of structures subjected to moving loads, Journal of Sound and Vibration 99 (1) (1985) 1-12.

[7] S.-I. Suzuki, Dynamic behavior of a finite beam subjected to travelling loads with acceleration, Journal of Sound and Vibration 55(1) (1977), 65–70.

[8] D. Yadav, Non-stationary dynamics of train and flexible track over inertial foundation during variable velocity, Journal of Sound and Vibration 147(1) (1991), 57–71.

[9] Anders Karlstrom, An analytical model for ground vibrations from accelerating trains, Journal of Sound and Vibration 293 (2006), 587–598.

[10] S. Krenk, L. Kellezi, S. R. K. Nielsen and P. H. Kirkegaard, Finite elements and transmitting boundary conditions for moving loads, Proceedings of the 4th European Conference on Structural Dynamics, Eurodyn '99, Praha, June 7-1, Vol. 1 (1999) 447-452

[11] L. Andersen, S. R. K. Nielsen and P. H. Kirkegaard, Finite element modelling of infinite Euler beams on Kelvin foundations exposed to moving loads in convected co-ordinates, Journal of Sound and Vibration 241 (4) (2001) 587-604.

[12] C.G. Koh, J.S.Y. Ong, D.K.H. Chua, J. Feng, Moving Element for Train-Track Dynamics, International Journal for Numerical Methods in Engineering 56 (2003), 1549-1567.

[13] C.G. Koh, P.P. Sze, T.T. Deng, Numerical and analytical methods for in-plane dynamic response of annular disk, International Journal of Solids and Structures 43 (2006) 112-131.

[14] C.G. Koh, G.H. Chiew, C.C. Lim, J. A numerical method for moving load on continuum, Journal of Sound and Vibration 300 (2007), 126-138.

[15] Ang Kok Keng, Dai Jian, Tran Minh Thi, Analysis of high-speed rail accounting for jumping wheel phenomenon, The International Conference on Advances in Computational Mechanics (ACOME), August 14-16, 2012, Ho Chi Minh City, Vietnam.

[16] Nielsen, J. C. O. and Abrahamsson, T. J. S, Coupling of physical and modal components for analysis of moving non-linear dynamic systems on general beam structures, International Journal for Numerical Methods in Engineering 33 (1992), 1843-1859

[17] C. Esveld, Modern Railway Track (2nd Edition). MRT Productions: Duisburg, 2001.

[18] Bathe, K. J., Finite Element Procedures, Prentice-Hall, Englewood Cliffs, N.J. (1996).

[19] S. G. Newton, R. A. Clark, An investigation into the dynamic effects on the track of wheel flats on railway vehicles, Journal Mechanical Engineering Science 21 (1979) 287-297.

[20] S.H. Ju, J.R. Liao, Error study of rail/wheel point contact method for moving trains with rail roughness, Computers and Structures 88 (2010) 813–824.